Published OnlineFirst October 11, 2011; DOI: 10.1158/0008-5472.CAN-11-1154

Integrated Systems and Technologies

Cancer Research

Metabolomic Profiling Reveals Potential Markers and Bioprocesses Altered in Bladder Cancer Progression

Nagireddy Putluri[1], Ali Shojaie[8], Vihas T. Vasu[3,6], Shaiju K. Vareed[1], Srilatha Nalluri[3,6], Vasanta Putluri[1], Gagan Singh Thangjam[3,6], Katrin Panzitt[1], Christopher T. Tallman[9], Charles Butler[10], Theodore R. Sana[11], Steven M. Fischer[11], Gabriel Sica[10], Daniel J. Brat[10], Huidong Shi[2,6], Ganesh S. Palapattu[2], Yair Lotan[12], Alon Z. Weizer[9], Martha K. Terris[4,6,7], Shahrokh F. Shariat[13], George Michailidis[8], and Arun Sreekumar[1,5]

Abstract

Although alterations in xenobiotic metabolism are considered causal in the development of bladder cancer, the precise mechanisms involved are poorly understood. In this study, we used high-throughput mass spectrometry to measure over 2,000 compounds in 58 clinical specimens, identifying 35 metabolites which exhibited significant changes in bladder cancer. This metabolic signature distinguished both normal and benign bladder from bladder cancer. Exploratory analyses of this metabolomic signature in urine showed promise in distinguishing bladder cancer from controls and also nonmuscle from muscle-invasive bladder cancer. Subsequent enrichment-based bioprocess mapping revealed alterations in phase I/II metabolism and suggested a possible role for DNA methylation in perturbing xenobiotic metabolism in bladder cancer. In particular, we validated tumor-associated hypermethylation in the cytochrome P450 1A1 (*CYP1A1*) and cytochrome P450 1B1 (*CYP1B1*) promoters of bladder cancer tissues by bisulfite sequence analysis and methylation-specific PCR and also by *in vitro* treatment of T-24 bladder cancer cell line with the DNA demethylating agent 5-aza-2′-deoxycytidine. Furthermore, we showed that expression of CYP1A1 and CYP1B1 was reduced significantly in an independent cohort of bladder cancer specimens compared with matched benign adjacent tissues. In summary, our findings identified candidate diagnostic and prognostic markers and highlighted mechanisms associated with the silencing of xenobiotic metabolism. The metabolomic signature we describe offers potential as a urinary biomarker for early detection and staging of bladder cancer, highlighting the utility of evaluating metabolomic profiles of cancer to gain insights into bioprocesses perturbed during tumor development and progression. *Cancer Res; 71(24); 7376–86. ©2011 AACR.*

Authors' Affiliations: [1]Departments of Molecular and Cell Biology, Verna and Marrs McLean Department of Biochemistry and Alkek Center for Molecular Discovery, Baylor College of Medicine; [2]Department of Urology, The Methodist Hospital, Houston, Texas; Departments of [3]Biochemisty, [4]Urology, [5]Surgery, and [6]Cancer Center, Georgia Health Science University; [7]Section of Urology, Charlie Norwood Veteran Affairs Medical Center, Augusta, Georgia; [8]Department of Statistics and [9]Urology, University of Michigan, Ann Arbor, Michigan; [10]Department of Pathology and Laboratory Medicine, Winship Cancer Institute, Emory University School of Medicine, Atlanta, Georgia; [11]Metabolomics Laboratory Application Group, Agilent Technologies, Santa Clara, California; [12]Department of Urology, University of Texas Southwestern Medical Center, Dallas, Texas; and [13]Department of Urology, Weill Medical College of Cornell University, New York, New York

Note: Supplementary data for this article are available at Cancer Research Online (http://cancerres.aacrjournals.org/).

N. Putluri, A. Shojaie, and V.T. Vasu contributed equally to this study.

Current address for A. Shojaie: Department of Biostatistics, University of Washington, Seattle, WA.

Current address for V.T. Vasu: Department of Medicine, Division of Oncology, National Jewish Health, Denver, CO.

Corresponding Author: Arun Sreekumar, Department of Molecular and Cellular Biology, Verna and Marrs McLean Department of Biochemistry and Alkek Center for Molecular Discovery, R 509, Margaret A Alkek Cancer Research Building, Baylor College of Medicine, Houston, TX 77030. Phone: 713-798-3304; Fax: 713-798-8711; E-mail: sreekuma@bcm.edu

doi: 10.1158/0008-5472.CAN-11-1154

Introduction

Bladder cancer is the fourth most common cancer in American men and accounts for more deaths annually in women than cervical cancer (1). Diagnosis and surveillance of bladder cancer currently consists of cystoscopy, aided by cytology and biopsy. Cystoscopy identifies most papillary and sessile lesions but may have low sensitivity for high-grade superficial disease (i.e., CIS); further cystoscopy may be associated with a high psychologic burden for some patients, particularly when coupled with biopsy (2). Although urine cytology has reasonable sensitivity and specificity for the detection of high-grade bladder cancer, it has poor sensitivity for detecting low-grade tumors, ranging from 4% to 31% (3). There is an urgent need for noninvasive, objective, and accurate markers that are sensitive and specific for risk stratification. One method to achieve this goal is to identify and better understand the multiplex molecular events that regulate the onset and progression of this deadly disease.

The metabolomic studies on bladder cancer published to date include profiling urine specimens to identify benign controls from bladder cancer using mass spectral profiles with minimal compound identification (4, 5). Notably, these studies did not include external validation (6). Furthermore, they do

Published OnlineFirst October 11, 2011; DOI: 10.1158/0008-5472.CAN-11-1154

not provide insight into the biochemical processes that may be involved in bladder cancer development and progression. To address these issues, we employed a unique approach to (i) identify bladder cancer–associated metabolomic signatures, (ii) nominate potential candidate biomarkers, and (iii) uncover bioprocesses that could potentially alter precarcinogen metabolism.

Materials and Methods

Clinical samples

Flash frozen, pathologically verified bladder tissues were obtained from tumor banks at the Winship Cancer Center at Emory and Medical College of Georgia following approval of the respective Institutional Review Boards (IRB, Clinical information in Supplementary Tables S1 and S2). These included bladder cancer as well as benign adjacent tissues (i.e., histologically confirmed benign tissue from areas adjacent to the tumor). Gold standard normal bladder tissues (from individuals having no prior/current history of bladder cancer) were purchased from NDRI (National Disease Research Interchange, Philadelphia, PA). Clinically annotated urine samples were obtained either prior to transurethral resection of bladder tumor (TURBT) or cystectomy at the Georgia Health Sciences University and its affiliated Charlie Norwood Veteran Affairs Medical Center of Augusta (GHSU/CNVAMC, group 1), University of Michigan (UM, group 2), Weill Cornell Medical College (WCMC, group 3), and University of Texas Southwestern Medical Center (UTSW, group 4), following informed consent under IRB approved protocols (Refer Table 1 for overview of urine specimens used in this study and Supplementary Tables S3–S6 for clinical information).

Tissue metabolome extraction

Following harvest, bladder tissues were stored at −140°C in liquid nitrogen until analysis. For extraction of the metabolome, 25 mg of tissue was homogenized in 1:4 ice-cold water: methanol mixture containing an equimolar mixture of 11 standard compounds (Supplementary Table S7). This was followed by metabolic extraction using sequential application of ice-cold organic and aqueous solvents (water:methanol: chloroform:water; ratio 1:4:3:1), deproteinization and drying of the extract. The latter was resuspended in injection solvent and analyzed by liquid chromatography–coupled to mass spectrometry (LC-MS). Detailed procedural description of tissue metabolome extraction is given in the Supplementary Methods.

Sample preparation for urine

Following collection, urine specimens were spun and the supernatant was stored at −70 °C until analysis. Osmolarity of all urine samples was measured using MULTI-OSMETTE 2430 osmometer (Precision Systems Inc.) and values calibrated using standards as per the manufacturer's instruction. The osmolarity of the urine samples examined was restricted to 140 to 400 milliosmoles/liter, which was achieved by measuring out a defined volume of the urine prior to extraction. This was followed by the introduction of an equimolar mixture of 4 standard compounds ([15N] Tryptophan, [D4] Thymine, [15N] *N*-acetyl aspartic acid, and [D5] Glutamic acid) into the specimen and the mixture was dried under vacuum (Genevac EZ-2plus). Prior to analysis, all samples were resuspended in an identical volume of water: acetonitrile injection solvent (98:2) consisting of 0.1% formic acid prior to LC-MS analysis.

Liquid chromatography–mass spectrometry

The chromatographic separation of metabolites was done using either reverse-phase (RP) separation or aqueous normal-phase (ANP) separation online with Quadrupole-Time-Of-Flight (QTOF)/Triple Quadrupole (QQQ) mass spectrometers (both Agilent Technologies) as published in Putluri and colleagues (7) and described in detail in Supplementary Methods. As controls to monitor the profiling process, an equimolar mixture of 11 standard compounds (described under Tissue Metabolome Extraction in Supplementary Methods) and a characterized pool of mouse liver tissue were extracted and analyzed in multiple times tandem with the clinical samples. Two blank runs were interspersed between clinical samples to prevent carry over of metabolites. Parameters used to operate the mass spectrometers for unbiased (Q-TOF) and targeted analysis [QQQ, single reaction monitoring (SRM) transitions in Supplementary Table S8] of metabolites and associated data preprocessing methods were identical to our earlier study (7) and are described in Supplementary Methods.

Metabolites were identified from the preprocessed mass spectral data using a 1,000-compound metabolomic library,

Table 1. Overview of the specimens used to evaluate biomarker potential of bladder-associated metabolites in urine

Group number	Sample collection site	Total number of specimens	Controls	Bladder cancer	Training/ validation
1	Georgia Health Science University (GHSU)	26	13	13	Validation
2	University of Michigan (UM)	44	16	28	Training/validation
3	Weill Cornell Medical College (WCMC)	45	11	34	Validation
4	University of Texas Southwestern Medical Center (UTSW)	19	11	8	Validation

Published OnlineFirst October 11, 2011; DOI: 10.1158/0008-5472.CAN-11-1154

METLIN (Agilent Technologies), using both mass and retention time information, as described in Putluri and colleagues (7). In addition, a subset of compounds associated with bladder cancer was identified using targeted MS/MS analysis.

Metabolomic data analysis

Metabolites in the profiling data, with more than 75% missing values across samples were removed from the analysis. The remaining metabolites included 1,509, 510, and 55 compounds in unbiased positive (+) and negative (−) ionization and SRM data, respectively, resulting in 1,905 unique compounds (listed in Supplementary Table S9) across platforms from which 99 metabolites were named. For included metabolites, the distribution of proportion of missing values in bladder cancer and benign samples were examined, and missing measures in metabolites were imputed according to the adaptive procedure described in the Supplementary Methods. Imputed data from positive and negative ionization were $\log_2$ transformed and quantile normalized per sample using the R-package "limma" (8). To avoid bias because of the small number of compounds measured by SRM, median centering was employed instead of quantile normalization. Data obtained from different platforms were z-transformed and compared across samples. The data from different platforms were combined by averaging over duplicate samples for each compound. Hierarchical clustering was done using complete linkage with Pearson's correlation and heat maps were drawn using R-packages "gplot" (9). A permutation-based ($n = 10{,}000$) 2-sided t test coupled to false discovery rate (FDR) correction using procedure implemented in R-package "fdrtool" (ref. 10; for all metabolites) or that described in Benjamini and colleagues (ref. 11; for named metabolites), with FDR threshold of $q^* = 0.2$, was used to assess the association of each metabolite with the cancer status of the sample.

Data from urine samples were first normalized with respect to the osmolarity level of the sample and then median centered and normalized using the interquartile range. Partial least square discriminant analysis (PLS-DA) classification models with 2 principal components [R-packages "pls" (12) and "caret" (13)] were used to classify the benign and bladder cancer samples in different datasets, as well as Muscle-invasive and non-muscle–invasive samples in the UM data set. Cross-validation coupled with repeated random splitting ($n = 1{,}000$), as described in Supplementary Methods, was used to obtain reliable estimates of classification errors in the training data.

Cell culture and 5-aza-2′-deoxycytidine treatment

Bladder cancer cell line (T-24) was obtained from American Type Culture Collection (ATCC) tested per standards described by the ATCC Genuine Cultures by the vendor and grown per vendor´s instructions. All experiments were carried out within 6 months of procurement of these cells. The cells were seeded at a density of 1×10^5 cells per well in 6-well plates and exposed to culture media containing either dimethyl sulfoxide ($\leq 0.05\%$, controls) or 5 μmol/L Aza 24 hours after attachment, for a total duration of 2 days (48 hours). 5-Aza-2′-deoxycytidine (AZA) was replenished at 24-hour intervals. At the end of the treatment period, both AZA-treated or control cells were trypsinized, rinsed with PBS, pelleted, and stored at −80°C until further analyses.

Real-time PCR (Q-PCR) analysis

Total RNA and cDNA were made from frozen bladder–derived tissues (∼50 mg) or cell line pellets using methods described in Sreekumar and colleagues (14). QPCR for enzymes involved in the phase I and II metabolic pathway were done as described (14) using gene-specific oligonucleotide primers (Supplementary Table S10). The $-\Delta\Delta C_t$ method (15) was used to calculate relative changes in mRNA levels measured by the quantitative reverse transcriptase PCR (qRT-PCR) experiments, after normalizing the transcript levels of each gene by the levels of glyceraldehyde control (11) were used to assess the changes of expressions in different experimental conditions.

Bisulfite treatment and DNA sequencing

Genomic DNA was extracted from tissues and/or cell lines using DNA extraction kit (Qiagen Inc.) and bisulfite treated using EZ-DNA methylation gold kit (Zymo Research Inc.), both per manufacturer's instructions. Regions containing CpG islands on cytochrome P450 1A1 (*CYP1A1*) and cytochrome P450 1B1 (*CYP1B1*) promoters were PCR amplified using specific primers (synthesized by Integrated DNA Technologies) 5′-AAACTAACCCTTTAAAAACCCC-3′ (sense) and 5′-TTTTTAGGGGGTAGAGGTTAGG-3′ (antisense) for CYP1A1 and 5′-TTTTATTTGGTGAAGAGGAGGAGTA-3′ (sense) and 5′-CAACAACTTCATCCTAAACAAATTCT-3′ (antisense) for CYP1B1. The PCR product (191 bp of the *CYP1A1* promoter and 246 bp of the *CYP1B1* promoter) covered 9 and 14 CpG sites, respectively, located approximately 1,000 bp upstream of the transcription start site. The PCR conditions that were employed were as follows: 95°C for 5 minutes, 40 cycles of 95°C for 15 seconds, 55°C for 30 seconds, 72°C for 30 seconds, and a final extension at 72°C for 7 minutes. PCR products were gel eluted and subcloned into T/A cloning vector pCR4 (Invitrogen) using TOPO TA Cloning Kit as per manufacturer's instructions. The cloned products were sequenced by Molecular Cloning laboratories (MC Labs) using M13 reverse primer. The bisulfite sequences were analyzed using BiQ Analyzer (16).

Methylation specific PCR

Methyl specific PCR (MSP) was done on bisulfite-treated genomic DNA (described above) using the *CYP1A1* promoter–specific primers 5′-CGTGTGGTTTTTGTTTGC-3′ (sense) and 5′-GAAACAACGTCGAAAACA-3′ (antisense), to obtain a 123 bp product. The PCR conditions were 95°C for 5 minutes, 33 cycles of 95°C for 15 seconds, 48.8°C for 30 seconds, 72°C for 25 seconds, and a final extension at 72°C for 7 minutes followed by 4°C. Human methylated and unmethylated DNA purchased from Zymo Research Corp. served as positive and negative controls, respectively. Protocols published in Khan and colleagues (17) and described in Supplementary Methods were used to carry out immunoblot analysis of CYP1A1 and CYP1B1 in bladder tissues.

Published OnlineFirst October 11, 2011; DOI: 10.1158/0008-5472.CAN-11-1154

Results

Metabolomic profiling of bladder cancer

A total of 58 pathologically evaluated bladder tissues (benign adjacent $n = 27$ and bladder cancer $n = 31$; matched pairs $n = 25$, power 87%, Supplementary Table S1) were examined for their metabolomic profiles using LC-MS. The metabolome was separated using both RP and ANP chromatography and examined using Q-TOF and QQQ mass spectrometers employing positive (+) and negative (−) electrospray ionization. The Q-TOF analysis involved unbiased profiling, whereas the QQQ was used to examine a focused set of 55 compounds using SRM (refer Supplementary Table S8 for a list of SRM transitions). Figure 1A and Supplementary Fig. S1 provide an overview of the metabolomics profiling and associated data analysis strategy employed in this study. Both the chromatographic separation of metabolites and their analysis by MS were monitored for drifts using internal standards (see Supplementary Methods) and biological replicates of pooled extract of mouse liver and were highly reproducible (CV $\leq$5%, Fig. 1B).

A total of 2,019 entities were detected using this robust platform, across the 58 biospecimens (Fig. 1C), of which 1,905 compounds were unique (Supplementary Table S9). Among these, 99 compounds were identified using a combination of database search and MS/MS (Fig. 1D).

Bladder cancer–associated metabolic profiles

A total of 459 of 1,905 metabolites were differential between bladder cancer and benign adjacent bladder tissue after multiple comparison adjustment at an FDR level of 20%. These included 50 named compounds that were altered in bladder cancer compared with adjacent benign tissues (Fig. 2A). Among the perturbed metabolites were elevated levels of aliphatic amino acids, namely serine, asparagine, and valine or their aromatic counterparts, namely tryptophan, phenylalanine, and histidine. There were also hydroxylated metabolites such as 3-hydroxy-kyneurenine, 4-hydroxy phenyl lactic acid, and 5-hydroxy indole acetic acid in the bladder cancer–associated compendia. Furthermore, levels of S-adenosyl methionine (SAM) were also elevated in bladder cancer tissues. Apart from these metabolites, bladder cancer tissues also had higher levels of aniline, a xenobiotic compound known to be involved in bladder carcinogenesis (18, 19), whereas levels of palmitic, lauric, and oleic acids were decreased in bladder cancer compared with adjacent benign tissues.

We examined 50-named bladder cancer–associated metabolites (Fig. 2A) in a distinct set of 50 pathologically confirmed bladder tissues ($n = 13$ matched bladder cancer and benign adjacent pairs and $n = 24$ normal bladder tissues, Supplementary Table S2), using a targeted SRM-based approach. A total of 39 of 50 bladder cancer–associated metabolites were measured with certainty in these independent tissues, with alterations in 35 of 39 compounds remaining significant in bladder cancer, compared with normal controls (Fig. 2B). Among these 35 compounds, levels of 31 corroborated the results in the prior profiling study (Fig. 2A). The remaining 4 compounds, namely hippuric acid, oleic acid, 4-pyridoxic acid, and pipecolic acid, which were modestly elevated in bladder cancer compared with adjacent benign tissue (Fig. 2A, profiling data), were found to be significantly reduced in tumors compared with normal bladder tissues (Fig. 2B). This opposing trend in expression observed when normal bladder specimens are used as controls, indicate the existence of a subtle "field effect" (20) in the benign adjacent tissues that were used in the profiling study. Therefore in light of this, our metabolic signature for bladder cancer consists of 35 named compounds from the "discovery profile" (Fig. 2A) that were also significant in the comparison between normal bladder and bladder cancer tissues (Fig. 2B). Notably, unsupervised hierarchical clustering of bladder tissues using these metabolites distinguished bladder cancer from benign adjacent and normal bladder controls (Fig. 2B), as well as delineated benign adjacent tissue from normal bladder controls with the misassignment of only 4 normal bladder tissues (Fig. 2B). Furthermore, when examined in prostate cancer specimens (10 benign cancer pairs), only 5 of 35 bladder cancer–associated compounds had nominal *P*-value below 0.05 (Supplementary Fig. S2), and only glyceraldehyde-3-phosphate was found significant after multiple comparison adjustment at 20% FDR level.

Evaluation of biomarker potential of bladder cancer–associated metabolites in urine

The classification power of bladder cancer–associated metabolites in tissues motivated us to investigate their biomarker potential in urine. We used 134 urine specimens collected independently at 4 institutions as described under Methods. In group 1 (GHSU/CNVAMC), specimens were collected from bladder cancer patients ($n = 13$) immediately prior to radical cystectomy ($n = 7$) or TURBT ($n = 6$), with or without prior intravesical immuno/chemotherapy and, age-matched control individuals ($n = 13$) with no history of cancer [e.g., neurogenic bladder ($n = 2$) or removal of kidney stones ($n = 10$), Supplementary Table S3]. In groups 2 (UM) and 3 (WCMC), specimens were collected from bladder cancer patients with or without any prior immuno/chemotherapy followed by cystoscopy, with urine collection before cystoscopy (Supplementary Tables S4 and S5). Here, patients were categorized as benign (responders to therapy or pT0) or bladder cancer (nonresponders to therapy). Individuals with suspicious cystoscopy findings were evaluated with TURBT. All histology slides from cystectomy specimens were reviewed and staged by a genitourinary pathologist without knowledge of the metabolomic data. In group 4 (UTSW), specimens were collected from bladder cancer patients ($n = 9$) prior to TURBT or cystectomy and controls were from age-matched control individuals ($n = 11$) with no history of bladder cancer (Supplementary Table S6). Specifically, the controls for our urine study contained benign controls in groups 2 and 3, who had a prior history of bladder cancer, but were considered disease free or benign after treatment, whereas the controls in the groups 1 and 4 had no prior history of bladder cancer.

Using a SRM-based approach (Supplementary Table S8 for SRM transitions), we could measure 25 of 35 tissue-derived

Published OnlineFirst October 11, 2011; DOI: 10.1158/0008-5472.CAN-11-1154

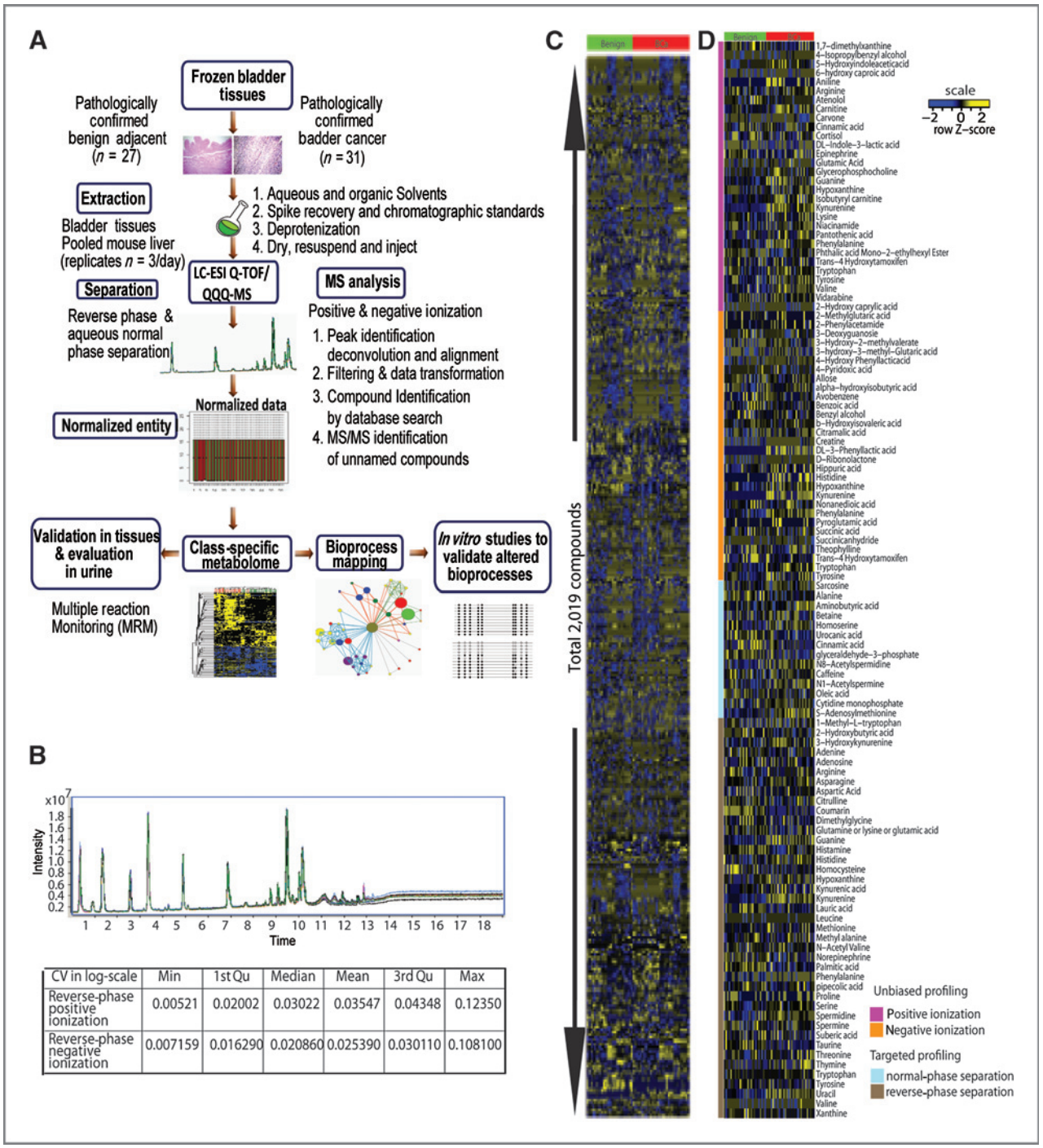

CV in log-scale	Min	1st Qu	Median	Mean	3rd Qu	Max
Reverse-phase positive ionization	0.00521	0.02002	0.03022	0.03547	0.04348	0.12350
Reverse-phase negative ionization	0.007159	0.016290	0.020860	0.025390	0.030110	0.108100

Figure 1. Metabolomic profiling of bladder cancer. A, overview of the strategy used to profile and characterize the metabolome of bladder cancer. B, chromatographic reproducibility of a mixture of 11 metabolite standards over 10 technical replicates identified on the Q-TOF using positive ionization (top) and a table showing the coefficient of variation (CV) for detection of 142 metabolites across 23 biological replicates of pooled liver extract. C, heat map of hierarchical clustering of 2,019 metabolites detected across 58 bladder-related samples. Columns represent individual tissue samples and rows refer to distinct metabolites. Shades of yellow represent elevation of a metabolite and shades of blue represent a decrease of a metabolite relative to the median metabolite levels (see scale). D, same as C, but for 99 named compounds identified across 58 bladder-related tissue specimens.

bladder cancer–associated metabolites in urine specimens collected at the 4 institutions. These 25 metabolites were altered in urine of bladder cancer patients compared with control urine from individuals having no history of bladder cancer (Supplementary Fig. S3). The reproducibility of these 25-metabolite measurements in urine was ascertained by independent replicate analysis of 10 specimens, which gave a Pearson Correlation of 0.965 to 0.995 (Supplementary Fig. S4).

Published OnlineFirst October 11, 2011; DOI: 10.1158/0008-5472.CAN-11-1154

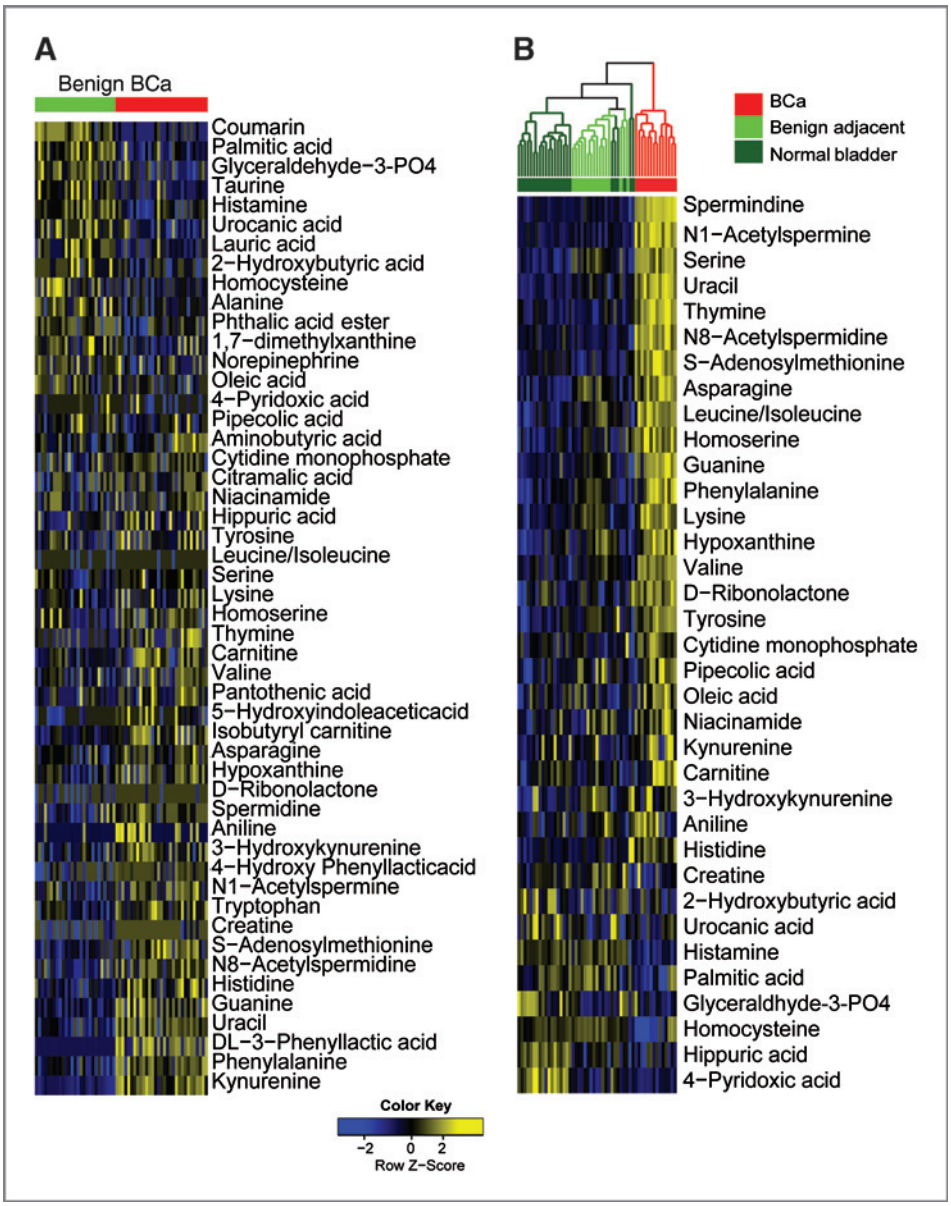

Figure 2. Metabolomic alteration in bladder cancer. A, heat map showing 50 named differential metabolites in bladder cancer relative to benign samples. B, heat map showing unsupervised hierarchical classification of an independent set of 50 bladder-derived tissues using 35 bladder cancer–derived significant compounds nominated by metabolic profiling studies. The color scheme for the heat maps is the same as in Fig. 1C.

We then examined the ability of these 25 metabolites to distinguish benign from bladder cancer in urine specimens using a PLS-DA with 2 principal components as described in Methods and illustrated in Fig. 3A. Supplementary Fig. S5 shows the 25 bladder cancer -associated metabolites contributed differently to the 2 principal components that together defined the classificatory power of the model. The receiver operator characteristic curve (ROC) for this classifier in training data from group 2 had an area under the curve (AUC) of 0.67 (90% CI: 0.52–0.83; Fig. 3B). When applied to independent test samples from group 1 ($n = 26$), group 3 ($n = 45$), and group 4 ($n = 19$), the classifier gave an AUC of 0.79, 0.62, and 0.76, respectively, in delineating benign and bladder cancer (Fig. 3B). In addition, a 2-stage model (Fig. 3A), successively combining urine cytology with the metabolic panel showed an improved AUC of 0.76 and 0.7 in classifying benign and bladder cancer specimens in groups 2 and 3, respectively (Fig. 3C). Furthermore, in a pilot study, an independent cross-validated PLS-DA model (refer Supplementary Fig. S6 for relative contribution of the metabolites), the 25-metabolite signature was able to distinguish muscle-invasive ($n = 8$) from noninvasive bladder cancer ($n = 20$) in group 2 specimens, with an AUC of 0.84 (90% CI: 0.63–0.94, Fig. 3D).

Integrative molecular concept modeling of bladder cancer progression

We examined whether bladder cancer–associated metabolites might be associated with altered biochemical processes fundamental to bladder cancer development and progression using oncomine concept maps (OCM), as described earlier (21).

Published OnlineFirst October 11, 2011; DOI: 10.1158/0008-5472.CAN-11-1154

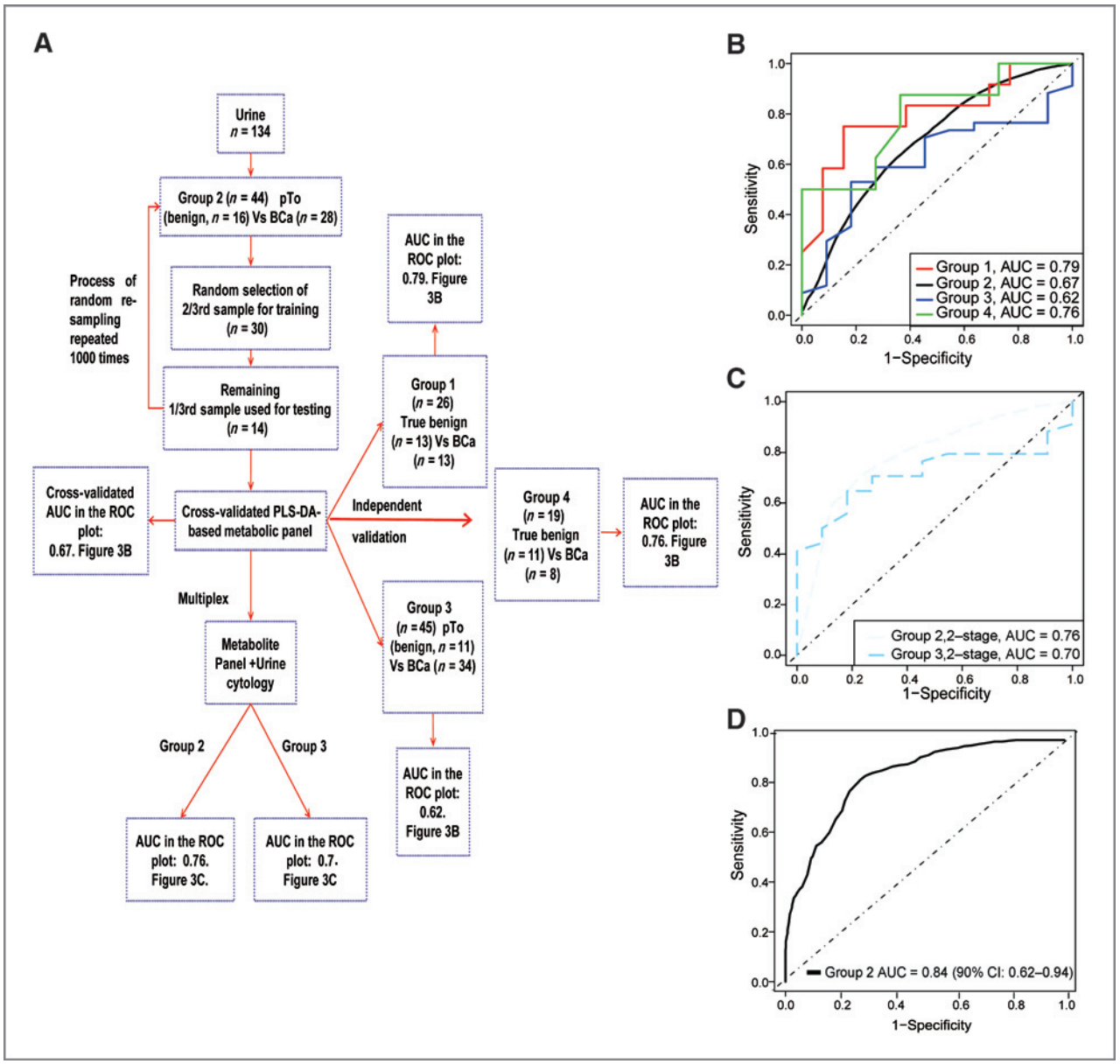

Figure 3. Biomarker potential of bladder cancer–associated metabolites in urine. A, overview of the strategy used to develop and validate the PLS-DA–based metabolomic model for delineating benign and bladder cancer in urine. B, ROC curve describing the ability of PLS-DA model using 25 bladder cancer –associated metabolites (M) to delineate benign and bladder cancer in urine. C, same as in B, but for combination of bladder cancer–associated metabolites (M) and urine cytology (UC) in delineating benign and bladder cancer in urine. D, same as in B, but for muscle-invasive ($n = 8$) and nonmuscle invasive ($n = 20$) bladder cancer in group 2 (UM cohort). BCa, bladder cancer.

OCM compares the information within the bladder cancer–associated metabolome with different biological concepts represented by molecular signatures also known as molecular concepts (i.e., lists of genes, proteins etc; ref. 21). Here, OCM analysis of the bladder cancer–associated metabolic signature was carried out using genes associated with metabolic pathways in *Homo sapiens* and listed in KEGG (http://www.genome.jp/kegg) as the null set and following the method described in Putluri and colleagues (7) and outlined in Supplementary Methods. A FDR threshold of 10% was used to select concepts of potential interest, all of which are listed in Supplementary Table S11 with a subset displayed in Fig. 4A.

The results of the OCM analysis validated our earlier prediction of altered amino acid metabolism in these specimens described in Fig. 2A. The enriched concepts (Fig. 4A) included those that described altered utilization of amino acids (i.e., methionine) and their aromatic counterparts (i.e., tyrosine and tryptophan), as well as metabolism of fatty acids, lactic acid, intermediates of tricarboxylic acid cycle, and electron transport. In addition to these, the bladder cancer–associated metabolomic profile also enriched for 2 additional biological

Published OnlineFirst October 11, 2011; DOI: 10.1158/0008-5472.CAN-11-1154

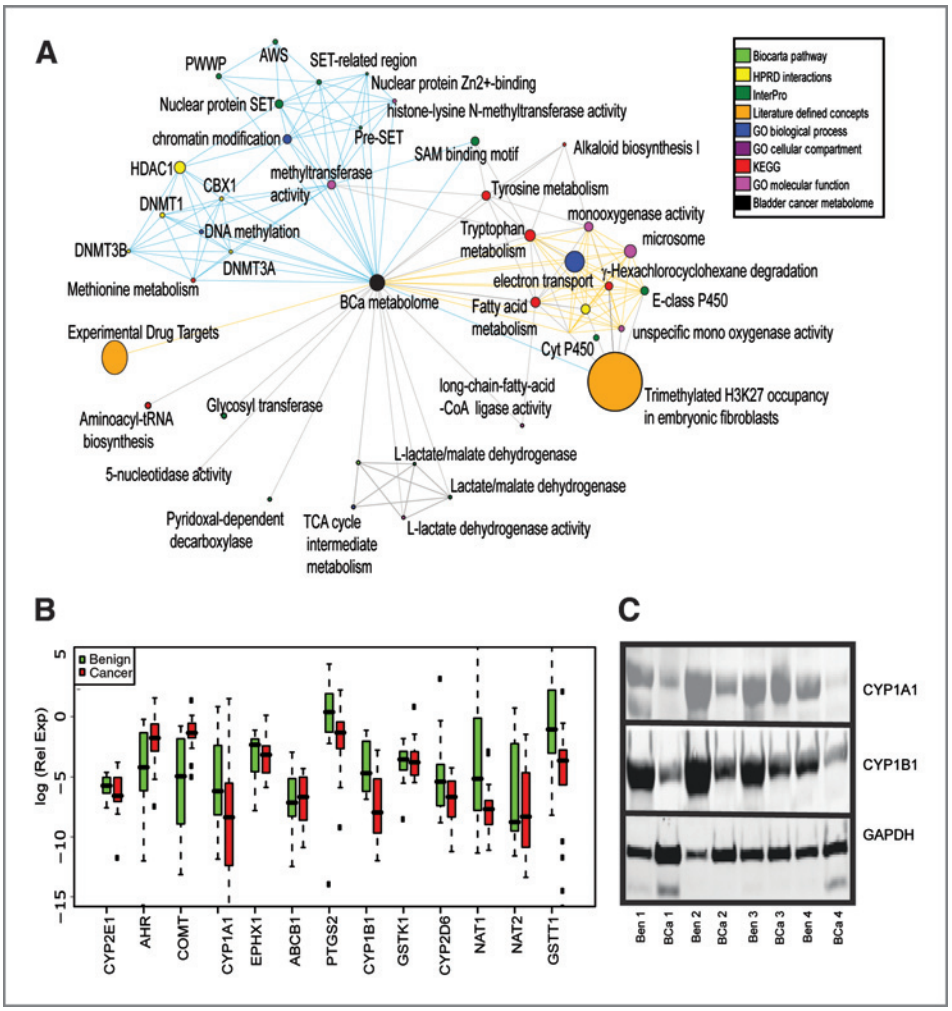

Figure 4. Cytochrome-driven xenobiotic metabolism is altered in bladder cancer. A, network view of the molecular concept analysis for the metabolomic profiles of our "bladder cancer–associated metabolic signature" (black node). Each node represents a molecular concept or a set of biologically related genes. The node size is proportional to the number of genes in the concept. Each edge represents a statistically significant enrichment (FDR $Q < 0.10$). Enriched concepts describing cytochrome P450-driven xenobiotic metabolism and methylation in bladder cancer indicated by yellow and blue edges, respectively. B, box plots for real-time PCR data showing relative transcript levels for enzymes in phase I/II metabolic pathway in matched bladder cancer (red) and adjacent benign tissues (green). C, immunoblot of CYP1A1 and CYP1B1 in bladder tumors compared with their matched benign adjacent tissues. BCa, bladder cancer; GAPDH, glyceraldehyde-3-phosphate dehydrogenase.

processes describing cytochrome P450-dependent xenobiotic metabolism and methylation. In our earlier study on prostate cancer, we described elevated methylation potential as a hallmark of aggressive prostate tumors (14). It is important to note that at least 39% of tumors we examined in our profiling experiments were muscle invasive and, hence, categorized as high-grade tumors (Supplementary Table S1). Furthermore, similar to our observation in prostate cancer (14), enriched methylation in bladder cancer may be a result of significantly elevated levels of the methyl donor SAM ($P = 1.71E-05$, FDR $Q < 2\%$), as well as methylated metabolites in tumor specimens compared with adjacent benign tissue (Fig. 2A). Notably, this enrichment of methylation potential in bladder cancer was described by multiple interconnected concepts describing DNA and histone methylation, chromatin modification, and involvement of SET domain containing proteins (Fig. 4A, blue bridges). Although this finding of perturbed methylation in bladder cancer tumors is consistent with other studies (22, 23), its coenrichment with the bioprocess describing altered cytochrome P40–mediated xenobiotic metabolism is intriguing (Fig. 4A, yellow bridges). Alteration in xenobiotic metabolism in bladder cancer, reflected in our data by elevated levels of aniline (Fig. 2A and B), has been attributed to be one of the causal factors for bladder cancer development (24–26), resulting from mutations in the genes programming phase I/II metabolic enzymes (25, 27–30). However, its coenrichment with methylaton leads us to hypothesize that epigenetic modification could also regulate the expression of phase I/II metabolic genes in bladder cancer.

To test this, we first examined the transcript levels for enzymes in phase I/II metabolism in matched bladder cancer and benign adjacent tissues ($n = 20$) using QPCR (primer sequence in Supplementary Table S10). The transcript levels for CYP1A1 and CYP1B1 were significantly reduced in bladder cancer tissues compared with benign adjacent tissues ($P < .01$, FDR $Q \leq 5\%$, Fig. 4B); a finding corroborated by reduced protein expression of CYP1A1 and CYP1B1 in bladder cancer (Fig. 4C) and justifying the OCM-based prediction of altered "cytochrome P450–dependent metabolism" in bladder tumors. Additional alterations included reduced transcript levels for cytochrome P450 2E1 (CYP2E1) and glutathione S-transferase T1 (GSTT1, both $P < 0.1$, FDR $Q \leq 20\%$), as well as higher mRNA levels for aromatic hydrocarbon receptor (AHR) and catechol-*O*-methyltransferase (COMT, $P < 0.001$, FDR $Q \leq 5\%$) in

Published OnlineFirst October 11, 2011; DOI: 10.1158/0008-5472.CAN-11-1154

bladder cancer tissues as compared with benign adjacent tissues (Fig. 4B).

To confirm the role of methylation in regulating the expression of phase I/II metabolic enzymes in bladder cancer tumors, we treated the bladder cancer cell line T-24 with the DNA methyl transferase inhibitor AZA (5 μm for 48 hours). AZA treatment resulted in a derepression of CYP1A1, 1B1, and EPHX1 (Fig. 5A) compared with untreated cells ($P < 0.01$ and FDR $Q \leq 5\%$, for all). Furthermore, bisulfite sequence analysis of these cells confirmed a 50% decrease in methylation of CpGs located approximately 1,000 bp upstream of the transcription start site on the *CYP1A1* promoter (Fig. 5B). In addition, bisulfite analysis and MSP confirmed hypermethylation of *CYP1A1* and *CYP1B1* promoters in 75% of patient-derived bladder tumors analyzed, compared with matched adjacent benign tissues (Fig. 5C–G). These results for the first time confirm a role for methylation as an alternate mechanism in regulating CYP1A1 and CYP1B1 expression in bladder cancer tumors.

Discussion

To understand bladder cancer development and progression, and to obtain insights into bioprocesses that could possibly be associated with defective xenobiotic metabolism, we conducted a MS-based comprehensive and unbiased metabolomic profiling of tissue specimens from bladder cancer

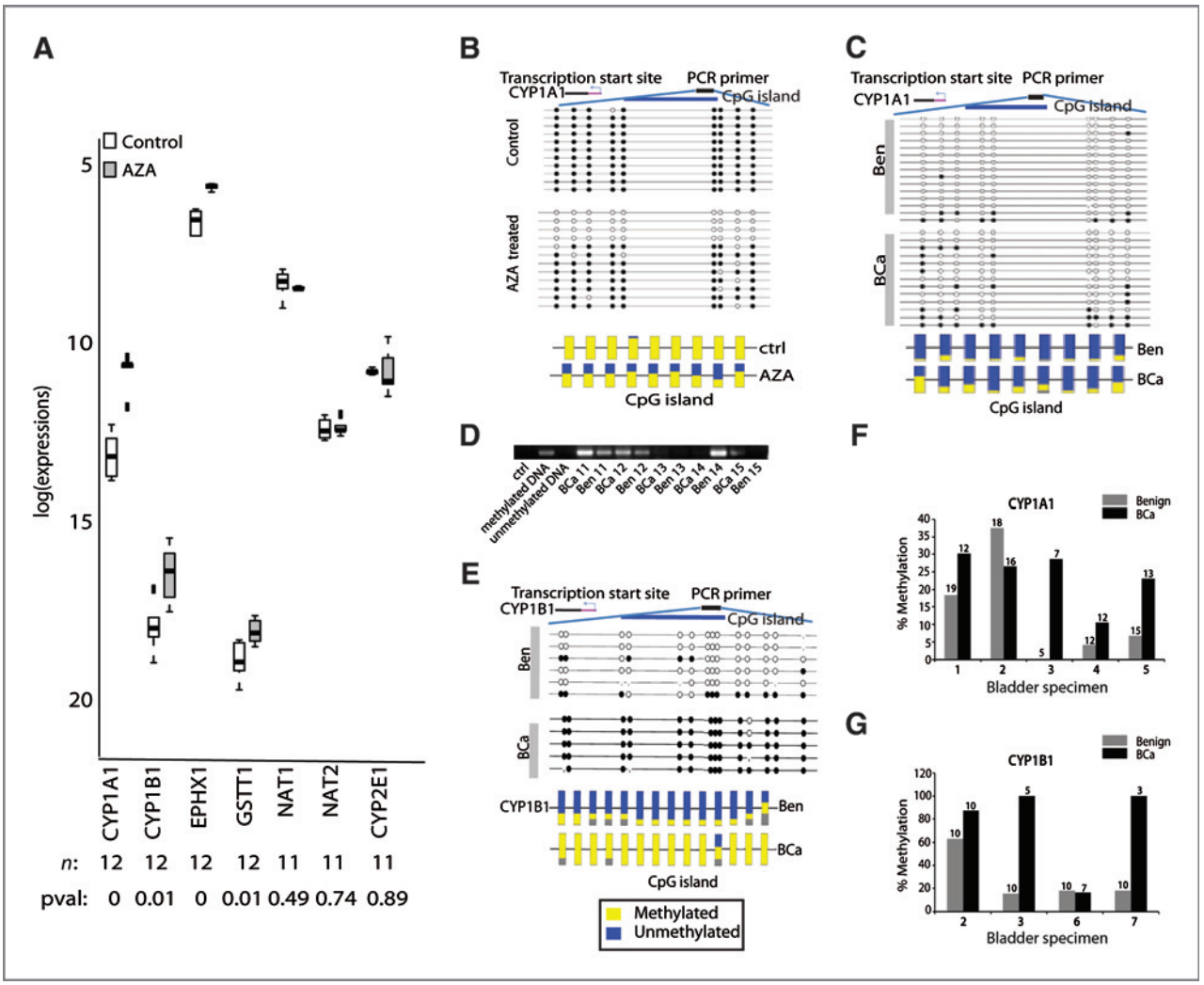

Figure 5. Methylation-induced silencing of phase I/II metabolic enzymes. A, box plots for real-time PCR data showing relative transcript levels in T-24 bladder cancer cells with and without treatment with 5-μm AZA. *n*, number of samples; pval, *P*-value. B, bisulfite sequencing of CYP1A1 in control and AZA-treated T24 bladder cancer cells. Each row indicates the methylation profile for the 9 CpG islands in an independent clone (top). Multiple clones were analyzed from the treated ($n = 11$) and untreated groups ($n = 12$). Filled circles indicate methylated cytosine and open circles denote the unmethylated residue (top). The bottom panel shows the average methylation profile for each CpG island. C, same as B, but for CYP1A1 in bladder cancer and matched benign adjacent tissue. D, methylation-specific PCR showing higher CpG methylation in *CYP1A1* promoter (product size = 127 bp) in matched bladder cancer and benign adjacent tissues ($n = 6$ pairs). E, same as B, but for CYP1B1 in bladder cancer and matched benign adjacent tissue. Methylation profile of 14 CpG islands was examined. F, plot summarizing the bisulfite sequence analysis results for *CYP1A1* promoter in bladder cancer and benign adjacent tissues. The median percentage methylation was calculated for each tissue using data obtained from all the sequenced clones. G, same as F, but for CYP1B1. BCa, bladder cancer.

Published OnlineFirst October 11, 2011; DOI: 10.1158/0008-5472.CAN-11-1154

patients and control individuals. Similar to our earlier observations in prostate cancer (14), the bladder cancer–associated metabolome is enriched with amino acids, confirming this metabolic process to be a consistent hallmark of tumor development. Furthermore, we observed that the bladder cancer–associated signature contains aromatic compounds and hydroxylated metabolic derivatives, both of which pinpoint aberrations in xenobiotic metabolism. Although these alterations have been previously reported, their occurrence in bladder cancer has been mainly attributed to defects in the genes regulating detoxification processes (28). However, using a data-driven approach, we confirmed a role for methylation as an additional contributing factor in regulating the expression of xenobiotic metabolizing enzymes. In addition to delineating mechanistic insights into bladder cancer development, our study also defines a compendium of metabolites that reliably distinguishes bladder cancer tissues from benign specimens, as well as in a pilot setting, delineates muscle-invasive and nonmuscle-invasive bladder cancer using patient-derived urine specimens. The PLS-DA–based classification model for detecting bladder cancer in urine had an overall accuracy between 67% and 72% in 4 independent cohorts (Fig. 3B). This is encouraging considering the benign controls in 2 of the cohorts were obtained from individuals with antecedent bladder cancer, who were in remission following immuno/chemotherapeutic treatment. These proof-of-concept studies set the stage for evaluating bladder cancer–associated metabolites as noninvasive markers to complement current diagnostic modalities with the goal of optimizing individual patient treatment selection.

In summary, this study describes the global metabolomic map for bladder cancer. Utilizing this approach, we have identified several potential markers for future development and have highlighted the importance of this technique in uncovering epigenetic alterations in genes (i.e., *CYP1A1* and *CYPB1*) involved in pathways implicated in bladder carcinogenesis.

Disclosure of Potential Conflicts of Interest

T.R. Sana and S.M. Fischer are employees of Agilent Technologies and hold stock options in the company. None of the other authors have any conflict of interest.

Acknowledgments

The authors thank Ravi Kolhe for help with pathology and Sitaram Gayathri for technical assistance.

Grant Support

This work is supported in part by the National Cancer Institute grant RO1CA13345 (A. Sreekumar), RO3CA139489-01 (A. Sreekumar) and RCA145444A (A. Sreekumar and G. Michailidis) and funds to A. Sreekumar from the Alkek Center for Molecular Discovery, Baylor College of Medicine and Georgia Cancer Coalition.

The costs of publication of this article were defrayed in part by the payment of page charges. This article must therefore be hereby marked *advertisement* in accordance with 18 U.S.C. Section 1734 solely to indicate this fact.

Received April 1, 2011; revised September 29, 2011; accepted October 5, 2011; published OnlineFirst October 11, 2011.

References

1. ACS. Cancer facts and figures 2010. American Cancer Society, Atlanta, GA; 2010.
2. van der Aa MN, Steyerberg EW, Sen EF, Zwarthoff EC, Kirkels WJ, van der Kwast TH, et al. Patients' perceived burden of cystoscopic and urinary surveillance of bladder cancer: a randomized comparison. BJU Int 2008;101:1106–10.
3. Lotan Y, Roehrborn CG. Sensitivity and specificity of commonly available bladder tumor markers versus cytology: results of a comprehensive literature review and meta-analyses. Urology 2003;61:109–18; discussion 18.
4. Pasikanti KK, Esuvanranathan K, Ho PC, Mahendran R, Kamaraj R, Wu Q, et al. Noninvasive Urinary metabonomic diagnosis of human bladder cancer. J Proteome Res 2010;9:2988–95.
5. Issaq HJ, Nativ O, Waybright T, Luke B, Veenstra TD, Issaq EJ, et al. Detection of bladder cancer in human urine by metabolomic profiling using high performance liquid chromatography/mass spectrometry. J Urol 2008;179:2422–6.
6. Shariat SF, Lotan Y, Vickers A, Karakiewicz PI, Schmitz-Drager BJ, Goebell PJ, et al. Statistical consideration for clinical biomarker research in bladder cancer. Urol Oncol 2010;28;389–400.
7. Putluri N, Shojaie A, Vasu VT, Nalluri S, Vareed SK, Putluri V, et al. Metabolomic profiling reveals a role for androgen in activating amino acid metabolism and methylation in prostate cancer cells. PLoS One 2011;6:e21417.
8. Smyth GK. Limma: linear models for microarray data'bioinformatics and computational biology solutions using R and bioconductor. In: Gentleman VC R, Dudoit S, Irizarry R, Huber W, editor. Bioinformatics and computational biology solutions using R and bioconductor. New York: Springer; 2005. p. 397–420.
9. Bolker B, Bonebakker L, Gentleman R, Huber W, Liaw A, Lumley T, et al. gplots: Various R programming tools for plotting data. In: Warnes GR, editor. R package version 2.8.0. ed; 2010.
10. Strimmer K. fdrtool: a versatile R package for estimating local and tail area-based false discovery rates. Bioinformatics 2008;24:1461–2.
11. Benjamini Y, Hochberg Y. Controlling the false discovery rate: a practical and powerful approach in multiple testing. J Roy Statist Soc 1995;Series B 57.
12. Wehrens RM, B.H. pls: Partial least squares regression (PLSR) and principal component regression (PCR). R package version 21-0 2007 [cited]. Available from: http://mevik.net/work/software/pls.html.
13. Wing J, Weston S, Wlliams A, Keefer C, Engelhardt A. caret: Classification and regression training. R package In: Kuhn M, editor. version 4.67. ed; 2010.
14. Sreekumar A, Poisson LM, Rajendiran TM, Khan AP, Cao Q, Yu J, et al. Metabolomic profiles delineate potential role for sarcosine in prostate cancer progression. Nature 2009;457:910–4.
15. Livak KJ, Schmittgen TD. Analysis of relative gene expression data using real-time quantitative PCR and the 2(-delta delta C(T)) method. Methods 2001;25:402–8.
16. Bock C, Reither S, Mikeska T, Paulsen M, Walter J, Lengauer T. BiQ analyzer: visualization and quality control for DNA methylation data from bisulfite sequencing. Bioinformatics 2005;21:4067–8.
17. Khan AP, Poisson LM, Bhat VB, Fermin D, Zhao R, Kalyana-Sundaram S, et al. Quantitative proteomic profiling of prostate cancer reveals a role for miR-128 in prostate cancer. Mol Cell Proteomics 2010;9:298–312.
18. Sepai O, Sabbioni G. Biomonitoring workers exposed to arylamines: application to hazard assessment. Adv Exp Med Biol 1996;387:451–5.

Published OnlineFirst October 11, 2011; DOI: 10.1158/0008-5472.CAN-11-1154

19. Carreon T, Hein MJ, Viet SM, Hanley KW, Ruder AM, Ward EM. Increased bladder cancer risk among workers exposed to o-toluidine and aniline: a reanalysis. Occup Environ Med 2010;67:348–50.
20. Jones TD, Wang M, Eble JN, MacLennan GT, Lopez-Beltran A, Zhang S, et al. Molecular evidence supporting field effect in urothelial carcinogenesis. Clin Cancer Res 2005;11:6512–9.
21. Rhodes DR, Kalyana-Sundaram S, Tomlins SA, Mahavisno V, Kasper N, Varambally R, et al. Molecular concepts analysis links tumors, pathways, mechanisms, and drugs. Neoplasia 2007;9:443–54.
22. Aleman A, Adrien L, Lopez-Serra L, Cordon-Cardo C, Esteller M, Belbin TJ, et al. Identification of DNA hypermethylation of SOX9 in association with bladder cancer progression using CpG microarrays. Br J Cancer 2008;98:466–73.
23. Vallot C, Stransky N, Bernard-Pierrot I, Herault A, Zucman-Rossi J, Chapeaublanc E, et al. A novel epigenetic phenotype associated with the most aggressive pathway of bladder tumor progression. J Natl Cancer Inst 2011;103;47–60.
24. Baris D, Karagas MR, Verrill C, Johnson A, Andrew AS, Marsit CJ, et al. A case-control study of smoking and bladder cancer risk: emergent patterns over time. J Natl Cancer Inst 2009;101:1553–61.
25. Altayli E, Gunes S, Yilmaz AF, Goktas S, Bek Y. CYP1A2, CYP2D6, GSTM1, GSTP1, and GSTT1 gene polymorphisms in patients with bladder cancer in a Turkish population. Int Urol Nephrol 2009;41:259–66.
26. Lower GM Jr, Nilsson T, Nelson CE, Wolf H, Gamsky TE, Bryan GT. N-acetyltransferase phenotype and risk in urinary bladder cancer: approaches in molecular epidemiology. Preliminary results in Sweden and Denmark. Environmental Health Perspectives; 1979:71–79. Int J Epidemiol 2007;36:11–8.
27. Fanlo A, Sinues B, Mayayo E, Bernal L, Soriano A, Martinez-Jarreta B, et al. Urinary mutagenicity, CYP1A2 and NAT2 activity in textile industry workers. J Occup Health 2004;46:440–7.
28. Grando JP, Kuasne H, Losi-Guembarovski R, Sant'ana Rodrigues I, Matsuda HM, Fuganti PE, et al. Association between polymorphisms in the biometabolism genes CYP1A1, GSTM1, GSTT1 and GSTP1 in bladder cancer. Clin Exp Med 2009;9:21–8.
29. Roos PH, Bolt HM. Cytochrome P450 interactions in human cancers: new aspects considering CYP1B1. Expert opinion on drug metabolism & toxicology 2005;1:187–202.
30. Thier R, Bruning T, Roos PH, Bolt HM. Cytochrome P450 1B1, a new keystone in gene-environment interactions related to human head and neck cancer? Arch Toxicol 2002;76:249–56.

Published OnlineFirst October 11, 2011; DOI: 10.1158/0008-5472.CAN-11-1154

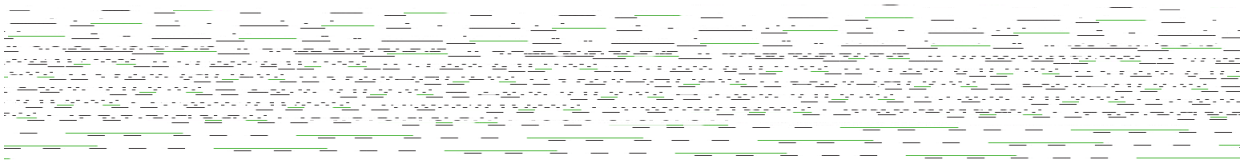

Metabolomic Profiling Reveals Potential Markers and Bioprocesses Altered in Bladder Cancer Progression

Nagireddy Putluri, Ali Shojaie, Vihas T. Vasu, et al.

Cancer Res 2011;71:7376-7386. Published OnlineFirst October 11, 2011.